An embedded interfacial network stabilizes inorganic halide perovskite

Abstract: The black perovskite phase of $CsPbI_3$ is promising for optoelectronic applications; however, it is unstable under ambient conditions, transforming within minutes into an optically inactive yellow phase, a fact that has so far prevented its widespread adoption. Here we use coarse photolithography to decompose and embed an endogenous PbI_2-based interfacial microstructure into otherwise-unstable $CsPbI_3$ perovskite thin films and devices. Films fitted with a tessellating microgrid are rendered resistant to moisture-triggered decay and exhibit enhanced long-term stability of the black phase (beyond 2.5 years in a dry environment), due to increasing the phase transition energy barrier and limiting the spread of potential yellow phase formation to structurally isolated domains of the grid. This stabilizing effect is readily achieved at the device level, where unencapsulated $CsPbI_3$ perovskite photodetectors display ambient-stable operation. Through *in situ* grazing incidence wide angle scattering (GIWAXS) experiments completed at the SNBL BM01 synchrotron beamline at ESRF, the improved thermal-phase stability is directly traced to the interface established in the polycrystalline thin film, a physical response verified by *ab initio* thermodynamic materials modelling. These findings provide insights into the nature of phase destabilization in emerging $CsPbI_3$ perovskite devices and demonstrates an effective stabilization procedure which is entirely orthogonal to existing approaches.

Goals: The key experimental observation required to complete our thermodynamic model was to directly observed the microgrid/perovskite interface, which acts as a strong stabilizing agent in the thin film. The crystal lattice of $CsPbI_3$ is relatively soft and prone to decompose when exposed to high energy beams, like those employed in electron microscopy experiments. Thus, rather than "zooming in" using microscopy, we aimed to capture the interface via its influence on the direction and distribution of grains (i.e. texture formation) within polycrystalline thin films embedded with the a microgrid.

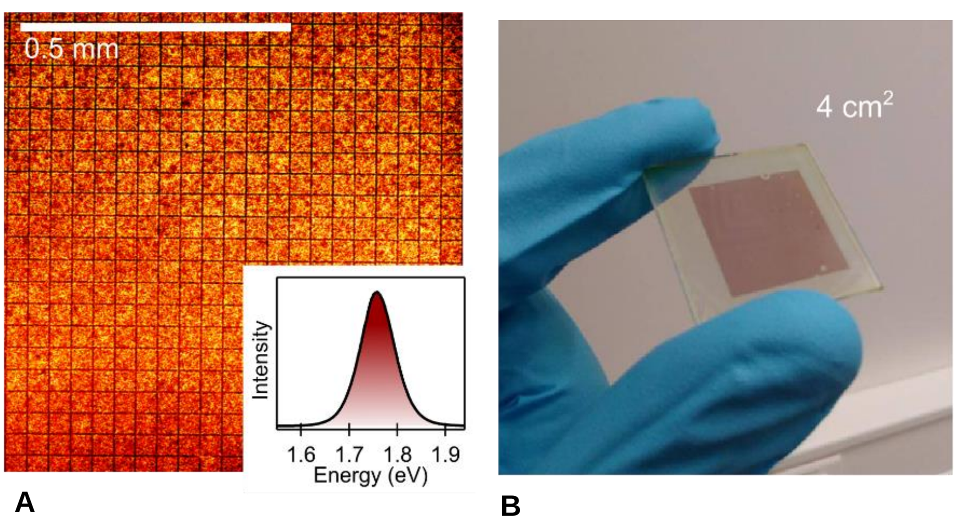

Figure 1| (A) Fluorescence micrograph of processed $CsPbI_3$ perovskite thin film (488 nm excitation / 695–705 nm detection), with a representative PL spectrum inset. (B) Photograph of an ambient-stable microgrid (40 µm) thin film after annealing.

Results: We embed a 3D network of anchoring sites into $CsPbI_3$ thin films to reinforce the desired, functional, perovskite phase. For this, we constructed a tessellating microgrid (Figure 1a) to form isolated micrometre domains of perovskite and we form films made up of these regions. We employed photolithography to pattern, using top-down (photo)thermal conversion of $CsPbI_3$ into local endogenous deposits of PbI_2. Increasing the size of the patterned area easily scales the process to stabilize whole films (Figure 1b).

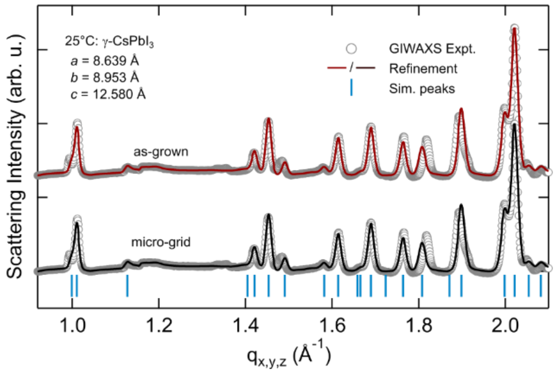

Figure 2| 1D GIWAXS patterns recorded from as-grown and processed black $CsPbI_3$ thin films (under N_2). Structural refinement (Le Bail method) confirms their common orthorhombic perovskite phase.

The optical properties of the stable perovskite surface are found to remain intact across the processed thin film and a common γ-CsPbI3 polycrystalline structure is preserved (Figure 2). However, 2D GIWAXS images reveal the subtle restructuring of the perovskite crystal when it interfaces with the embedded grid (Figure 2A). The normal polycrystalline thin film texture is altered by the microgrid, confirming additional anisotropy in the system. Taking the (200) peak as an example to make the point, Figure 3 shows how the smooth distribution of the as-grown film (Texture 1) departs when the microgrid is introduced (Texture 2), appearing more irregular, although always superimposing and amplifying narrow regions of Texture 1. The hot spots confirm the presence of a 3D interface throughout the grid.

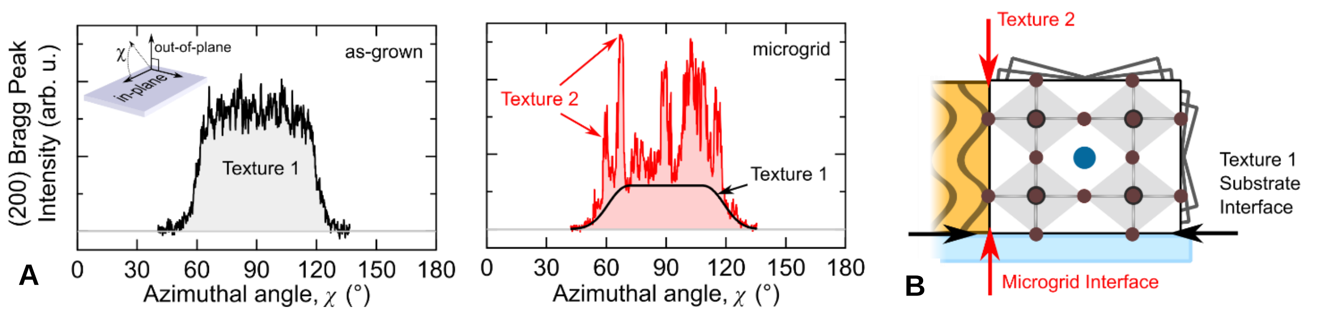

Figure 3| (A) GIWAXS intensity of (200) γ-$CsPbI_3$ scattering planes measured with and without a microgrid, as a function of azimuthal angle (χ). The inset illustrates the angle χ relative to the film plane. (B) Illustrations of the anisotropic origins of Textures 1 and 2.

Considering the relative intensity of the two texture components, a quantitative analysis (Figure 4) decouples the relative scattering volume from which they originate. We find that at least one third of the film grains are influenced by the anisotropy imposed by the microgrid and, assuming grains bordering the microgrid are most influenced, this suggests grains located far away from the boundary are also driven to express Texture 2. The embedded interface realized via the photolithography is the origin of the added anisotropy, leading directly to the strong stabilizing effect outlined in Figure 1. Using perovskite photodetectors as a conceptual demonstrator, we show how this approach offers a simple and effective strategy toward ambient processed and stable $CsPbI_3$ optical devices.

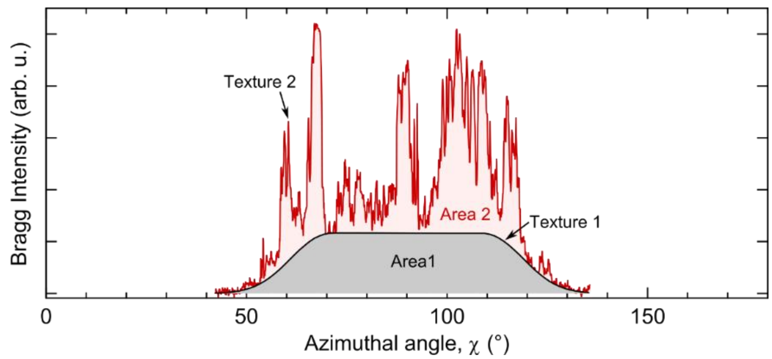

Figure 4| An evaluation of the relative X-ray scattering contributions arising from the overlap of Textures 1 and 2 recorded from a polycrystalline, black $CsPbI_3$ thin film processed with a 40 µm grid. The GIWAXS beam H×V profile is roughly 50×100 µm at an incident angle of 1°, meaning that the incident footprint encompasses many hundreds of grids. For a given azimuthal angle range, the area under the curve is assumed to be proportional to the scattering volume of crystal domains contributing to that particular texture expression. Texture 1 is shown to be an intrinsic expression of thermally treated $CsPbI_3$ thin film atop glass. Thus, subtracting the Area 1 lineshape from Area 2 we can estimate the relative population of grains influenced to additionally express Texture 2 (introduced by the micro-grid). Through this analysis we arrive at the relative ratio for Texture 1 and 2 of approximately 3:1, which is consistent across multiple samples processed with 40 µm grids. Note that Texture 2 will average out to Texture 1 with a larger enough beam size, this value thus represents the lower bound, with the true value being possibly higher.

Research outputs: This work was recently published in the high impact journal *Nature Communications* (impact factor = 14.92).

Steele, J. A. et al. An embedded interfacial network stabilizes inorganic $CsPbI_3$ perovskite thin films. Nat Commun 13, 7513 (2022).